ATMOSPHERIC SCIENCE LETTERS
*Atmos. Sci. Let.* (2014)
Published online in Wiley Online Library
(wileyonlinelibrary.com) **DOI:** 10.1002/asl2.523

RMetS
Royal Meteorological Society

# Direct effect of lower-tropospheric diabatic heating on surface wind over the equatorial Pacific

Lijuan Li,[1]* Bin Wang[1,2] and Tianjun Zhou[1]

[1]*State Key Laboratory of Numerical Modeling for Atmospheric Sciences and Geophysical Fluid Dynamics (LASG), Institute of Atmospheric Physics, Chinese Academy of Sciences, Beijing, China*
[2]*Ministry of Education Key Laboratory for Earth System Modeling, Center of Earth System Science (CESS), Tsinghua University, Beijing, China*

**Correspondence to:*
*L. Li, LASG, Institute of Atmospheric Physics, Chinese Academy of Sciences, No. 40, Hua Yan Li, Beijing 100029, China.*
*E-mail: ljli@mail.iap.ac.cn*

Received: 10 December 2013
Revised: 15 July 2014
Accepted: 21 July 2014

## Abstract

**The direct effect of lower-tropospheric diabatic heating (DH) on surface circulation over the equatorial Pacific is revealed using the theoretical analysis and three atmospheric general circulation model (AGCM) simulations, only differing their moist processes. The AGCM results suggest that the insensitivity of surface wind to DH in the middle and high levels is closely associated with the vertical disagreement of DH between the layers below and above 925 hPa over the equatorial Pacific.**

**Keywords:** **diabatic heating; surface wind; AGCM simulations**

## 1. Introduction

The surface winds have a profound influence on sea surface temperature (SST) through oceanic upwelling, mixing and surface latent heat (LH) flux to atmosphere over the equatorial Pacific and Atlantic, and vice versa. However, their accurate simulations are challenging for both atmospheric and coupled general circulation models (AGCM/CGCM) (e.g. Chang *et al.*, 2007; Guilyardi *et al.*, 2009). Two factors contributing to surface wind biases are generally considered: diabatic heating (DH) by both shallow convection and longwave radiation at low levels (850–700 hPa) and by cumulus convection at high levels, and SST gradients (Nigam and Chung, 2000; Chiang *et al.*, 2001; Wu, 2003; DeWitt, 2005; Zhang and Hagos, 2009). The vertical DH profiles, precipitation amounts and boundary layer entrainment are also thought to be the likely causes of surface wind biases (e. g. Schumacher *et al.*, 2004; Chang *et al.*, 2008; Zermeño-Diaz and Zhang, 2013). Except for SST gradients, all of the above causes indirectly affect the surface through changes in Walker (or Hadley) circulation or deduced circulation by the DH above surface.

On the other hand, the study on direct effect of lower-tropospheric DH, i.e. heating from physical processes such as radiation, cloud condensation, and turbulence, on surface wind is limited because of the difficulty to observe DH in atmosphere. Although DH could be estimated from reanalysis wind and temperature fields, there are large disagreements between these retrievals and the DH output directly from the reanalysis models in the tropics, especially in the lower troposphere (Chan and Nigam, 2009; Hagos *et al.*, 2010; Ling and Zhang, 2011, 2013; Wright and Fueglistaler, 2013). In theory, the tropical response to specified heating has been pioneered by Matsuno (1966) and Gill (1980) as follows:

$$\epsilon u - \frac{1}{2}yv = -\frac{\partial p}{\partial x} \tag{1}$$

$$\epsilon v + \frac{1}{2}yv = -\frac{\partial p}{\partial y} \tag{2}$$

$$\epsilon p + \frac{\partial u}{\partial x} + \frac{\partial v}{\partial y} = -Q \tag{3}$$

where $(x, y)$ is nondimensional distance with $x$ eastward and $y$ northward from equator, $(u, v)$ is proportional to the horizontal velocity, $p$ is proportional to the pressure perturbation, $Q$ is proportional to the heating rate, and $\epsilon^{-1}$ is a dissipation time scale. Combining Equations (2) and (3) with Equation (1), the above three equations can be reduced to a single equation,

$$\left(\epsilon + \frac{y^2}{4\epsilon}\right)u = \frac{1}{\epsilon}\frac{\partial Q}{\partial x} + \frac{y}{2\epsilon^2}\frac{\partial Q}{\partial y} + \frac{1}{\epsilon}\frac{\partial}{\partial x}\left(\frac{\partial u}{\partial x} + \frac{\partial v}{\partial y}\right) + \frac{y}{2\epsilon^2}\frac{\partial}{\partial y}\left(\frac{\partial u}{\partial x} + \frac{\partial v}{\partial y}\right) \tag{4}$$

As $\epsilon$ is positive, $u$ is directly affected by $\frac{\partial Q}{\partial X}$ and $y\frac{\partial Q}{\partial y}$, indicating the surface wind is directly modulated by the heating distribution. Hence, this study examines the direct effect of different horizontal distributions of DH in the lower troposphere on surface wind using three AGCM simulations.

## 2. Models and experiments

Two versions of the Grid-point Atmospheric Model of IAP (Institute of Atmospheric Physics) LASG

(National Key Laboratory of Numerical Modeling for Atmospheric Sciences and Geophysical Fluid Dynamics) (GAMIL), i.e. GAMIL1, the version for the Coupled Model Intercomparison Project (CMIP) Phase 3 (CMIP3), and GAMIL2, the version for the CMIP Phase 5 (CMIP5), are used in this study (Li and Wang, 2010; Li *et al.*, 2012, 2013a, 2013b). Both use a finite difference dynamical core that conserves mass and effective energy under the standard stratification approximation while solving the primitive hydrostatic equations of baroclinic atmosphere (Wang *et al.*, 2004), and a two-step shape-preserving advection scheme (TSPAS) for the moisture equation (Yu, 1994), with the same horizontal ($128 \times 60$) and vertical (26-$\sigma$) resolutions. Both estimate three types of clouds using the diagnostic Slingo-type scheme, namely, convective cloud, low-level marine stratus and layered cloud, and share the same shallow convection scheme, radiation, diffusion and boundary layer process.

The major differences between the two model versions are the cloud-related process schemes, for example, the deep convective parameterizations (Zhang and McFarlane, 1995; Zhang and Mu, 2005), convective cloud fraction (Xu and Krueger, 1991; Rasch and Kristjánsson, 1998) and cloud microphysical schemes (Rasch and Kristjánsson, 1998; Morrison and Gettelman, 2008), including the retuning of 14 uncertain parameters (for more details see Tables 1 and 2 in Li *et al.*, 2013b).

The model DH is defined as the sum of the heating rate from moist process (including shallow convection, deep convection and cloud macro-/micro-physical process), radiation and diffusion outputted by GAMILs. To obtain the different lower-tropospheric tropical heating and surface wind distributions, three sets of numerical experiments are performed, only differing their moist processes. The first two experiments use GAMIL1 and GAMIL2, respectively, of which the deep convection (including convective cloud) and cloud microphysics are different, and the third is identical to the second one except that the Hack scheme for shallow convection is turned off between 30°S and 30°N (referred to as GAMIL2-nosh) owing to the important role of shallow convection in tropical heating and tropical wind convergence in the lower troposphere (Zhang and Song, 2009; Cai *et al.*, 2013). Each experiment runs for 28 years from January 1975 to December 2002 forced with the same forcing data recommended by the CMIP5, such as the solar constant, greenhouse gases and Hadley Centre Sea Ice and Sea Surface Temperature data set (HadISST), and the last 24 years of the model output (1979–2002) are used for analyses and comparisons.

The National Centers for Environmental Prediction (NCEP) Reanalysis II (Kanamitsu *et al.*, 2002) and the European Centre for Medium-Range Weather Forecasts (ECMWFs) Interim Reanalysis (Simmons *et al.*, 2006) are used to evaluate the model results.

## 3. Results

The multi-year averaged annual mean zonal wind and DH at 850 and 1000 hPa over the equatorial Pacific are shown in Figure 1. GAMIL1 and GAMIL2 produce the almost identical easterly wind speed at 850 hPa, but the different strength at 1000 hPa over the central and eastern Pacific. At 850 hPa, the winds in GAMIL1 and GAMIL2 are stronger than those in both reanalysis datasets and GAMIL2-nosh between the dateline and 120°W (Figure 1(a)). Simulations of zonal wind are consistent with their distinct DH changes from west to east across the Pacific. Between 150°E and 180°E, the DH is about $0.8\,\mathrm{K\,day^{-1}}$ in GAMIL1 and GAMIL2, while about $0.1\,\mathrm{K\,day^{-1}}$ in GAMIL2-nosh; in the eastern Pacific, the diabatic cooling is from $-0.2\,\mathrm{K\,day^{-1}}$ in GAMIL2-nosh to $-0.5\,\mathrm{K\,day^{-1}}$ in GAMIL1 (Figure 1(b)). The weaker DH decreases eastwards (or negative gradients) in GAMIL2-nosh, the weaker easterlies in GAMIL2-nosh among three simulations. At 1000 hPa, the easterlies in GAMIL1 are about $3\,\mathrm{m\,s^{-1}}$ weaker than in GAMIL2 in the eastern of the dateline, and very close to two reanalyses and GAMIL2-nosh in the central Pacific (Figure 1(c)). Nonetheless, simulations of surface wind do not completely coincide with their DH changes (Figure 1(d)). On one hand, east of 150°W the heating at 1000 hPa increases with increased longitudes in three simulations are opposite to the negative observed SST gradients. The larger DH increases (or positive gradients) in GAMIL1, the smaller easterly winds in GAMIL1. This is consistent with Equation (4). On the other hand, the DH changes along longitudes in GAMIL2 and GAMIL2-nosh are nearly equal, while the differences of speed are very large, about $3\,\mathrm{m\,s^{-1}}$ near the dateline. Moreover, west of 150°W the DH increases along longitudes (positive gradients) in GAMIL1 are opposite to other two simulates and the observed SST gradients. However, the easterly winds in GAMIL1 are a little stronger than in GAMIL2-nosh and both reanalyses. Different $u$ with the same DH changes in the zonal direction by GAMIL2 and GAMIL2-nosh and strong easterlies west of 150°W in GAMIL1 with positive zonal DH gradients by GAMIL1 are not in accordance with Equation (4). Both imply the lack of considering the impacts of DH changes in the meridional direction on zonal wind perturbation. It should be noted that there is a spread of zonal wind in both reanalyses over the eastern equatorial Pacific, i.e. about $2\,\mathrm{m\,s^{-1}}$ underestimation at 850 hPa and $1\,\mathrm{m\,s^{-1}}$ overestimation at 1000 hPa in NCEP2 compared with ECMWF-interim (e.g. Back and Bretherton, 2006; Kumar *et al.*, 2013).

First, to understand the causes for the similar $u$ at 850 hPa and the different $u$ at 1000 hPa in GAMIL1 and GAMIL2, the vertical DH profiles are given (Figure 2). Obvious contrast between the heating in the western Pacific and the cooling in the eastern Pacific exists in three simulations from the middle (or upper, see Figure 13 in Li *et al.*, 2014) troposphere to about

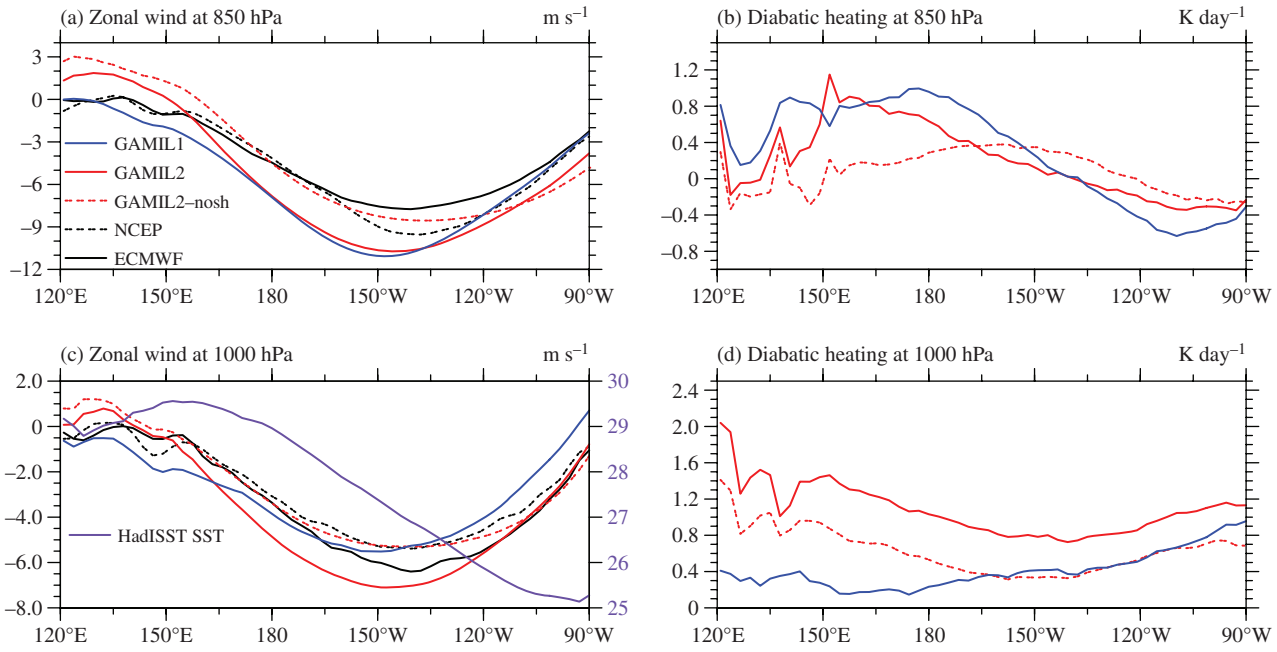


**Figure 1.** Annual mean zonal wind and diabatic heating at 850 and 1000 hPa and sea surface temperature (purple line-right scale) over the equatorial (5°S–5°N) Pacific.

925 hPa. The strong heating is from the LH release in the western convection centers, and the cooling is due to the longwave radiation in the eastern subsidence regions, where the LH is weak. There is a layer of strong LH between 850 and 925 hPa, where the longwave radiation cooling is also strong. However, such a contrast cannot be found below 925 hPa, where the positive DH is the smallest near 150°W and increases in both the eastern and western directions in GAMIL2 and GAMIL2-nosh, and increases eastwards in GAMIL1 (also seen in Figure 1). Below the 925-hPa level, the changes of total DH along longitudes are consistent with the distributions of evaporation cooling, more evaporation in the western Pacific and less evaporation in eastern Pacific, in GAMIL1, and of the diffusion heating and radiation cooling in GAMIL2 and GAMIL2-nosh. This disagreement of DH changes in the east–west direction above and below 925 hPa in GAMILs is also observed in other diagnosed DH based on the reanalysis and direct DH output of the Modern Era Retrospective Analysis for Research and Applications (MERRA), especially over the eastern equatorial Pacific (e.g. Figure 5 in Chan and Nigam, 2009; Figure 3 in Ling and Zhang, 2011). Furthermore, this vertical DH discrepancy may contribute to the different behaviors of zonal wind at 850 and 1000 hPa in GAMIL1 and GAMIL2, the same speed at 850 hPa in both and the stronger easterlies in GAMIL2 at 1000 hPa. In another aspect, if the surface winds mainly stem from the induced circulation by the DH above 850 hPa under the same SST, GAMIL1 and GAMIL2 would have the same zonal winds at 1000 hPa as at 850 hPa. Hence, the differences of zonal wind in GAMIL1 and GAMIL2 between at 850 hPa and at 1000 hPa suggest that the surface wind is not sensitive to DH above 850 hPa over the equatorial Pacific. The insensitivity of surface winds to the DH profiles is also noted over the equatorial Atlantic (Chang *et al.*, 2008; Zermeño-Diaz and Zhang, 2013). Moreover, both the same easterlies at 850 hPa and the different easterlies at 1000 hPa in GAMIL1 and GAMIL2, and the insensitivity of surface winds to DH in the middle and high levels are closely associated with the vertical DH discrepancies between the layers above and below 925 hPa over the equatorial Pacific. In addition, near the surface, the cooling in the moist and radiative processes is mostly counterbalanced by the diffusion heating, and thus the total DH is relatively small to three components. The cooling below 925 hPa in the moist process comes from the evaporation of deep convective and stratiform precipitation, partly offsetting by the weak heating from the shallow convection (figure not shown).

Second, to comprehensively understand the influence of DH on winds, the geographical distribution of DH and winds at 1000 hPa is displayed in Figure 3. The correspondence of the geographical differences of DH gradients and surface wind among three simulations conforms to the Equation (4). For instance, compared with GAMIL1, GAMIL2 produces the more DH in the western Pacific and off-equator, which result in the stronger easterlies along the equator, and southerly winds north of the equator, and northerly winds south of the equator. In comparison with GAMIL2-nosh, GAMIL2 overestimates the DH in the inter-tropical convergence zone (ITCZ) and south Pacific convergence zone (SPCZ) and underestimates the DH in the eastern equatorial Pacific and sub-tropics, which

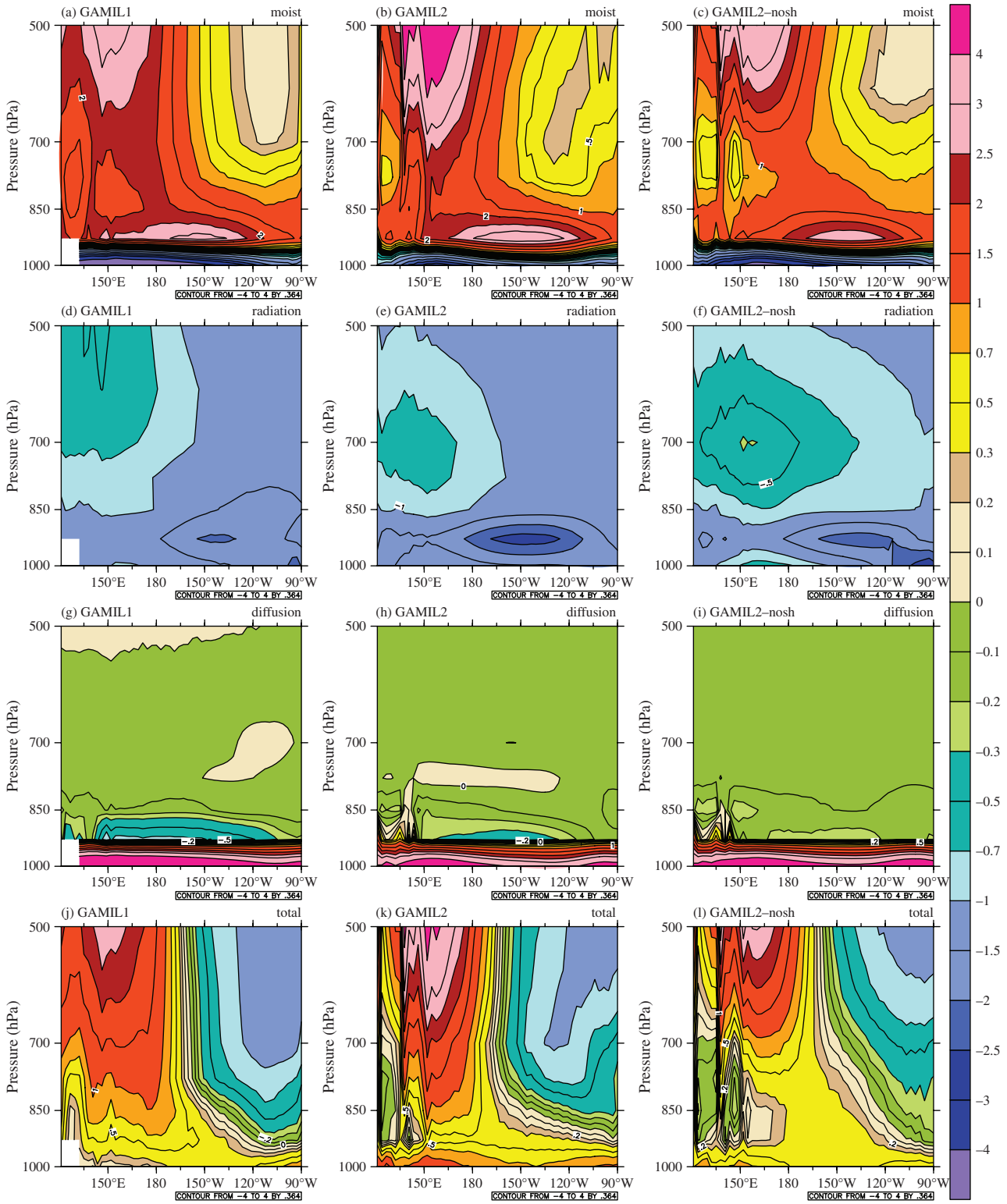


**Figure 2.** Vertical cross section of diabatic heating rate in (a–c) moist process, (d–f) radiation, (g–i) diffusion and (j–l) total physical processes for GAMIL1, GAMIL2 and GAMIL2-nosh; unit: K day$^{-1}$.

leads to easterly and southerly wind anomalies, especially over the central equatorial Pacific (rectangle in Figure 3(e)).

Additionally, the largest differences of DH among the simulations are near ITCZ and SPCZ, in accordance with the rainfall differences (Figure 4). Despite only differing the moist processes among the simulations, the rainfall differences between GAMIL2 and GAMIL1 are geographically similar to those between GAMIL2 and GAMIL2-nosh, more precipitation in the ITCZ and western equatorial Pacific in GAMIL2 than in both GAMIL1 and GAMIL2-nosh, indicating the important role of other physical processes, such as boundary layer and radiation, in rainfall simulations there. Hence, the

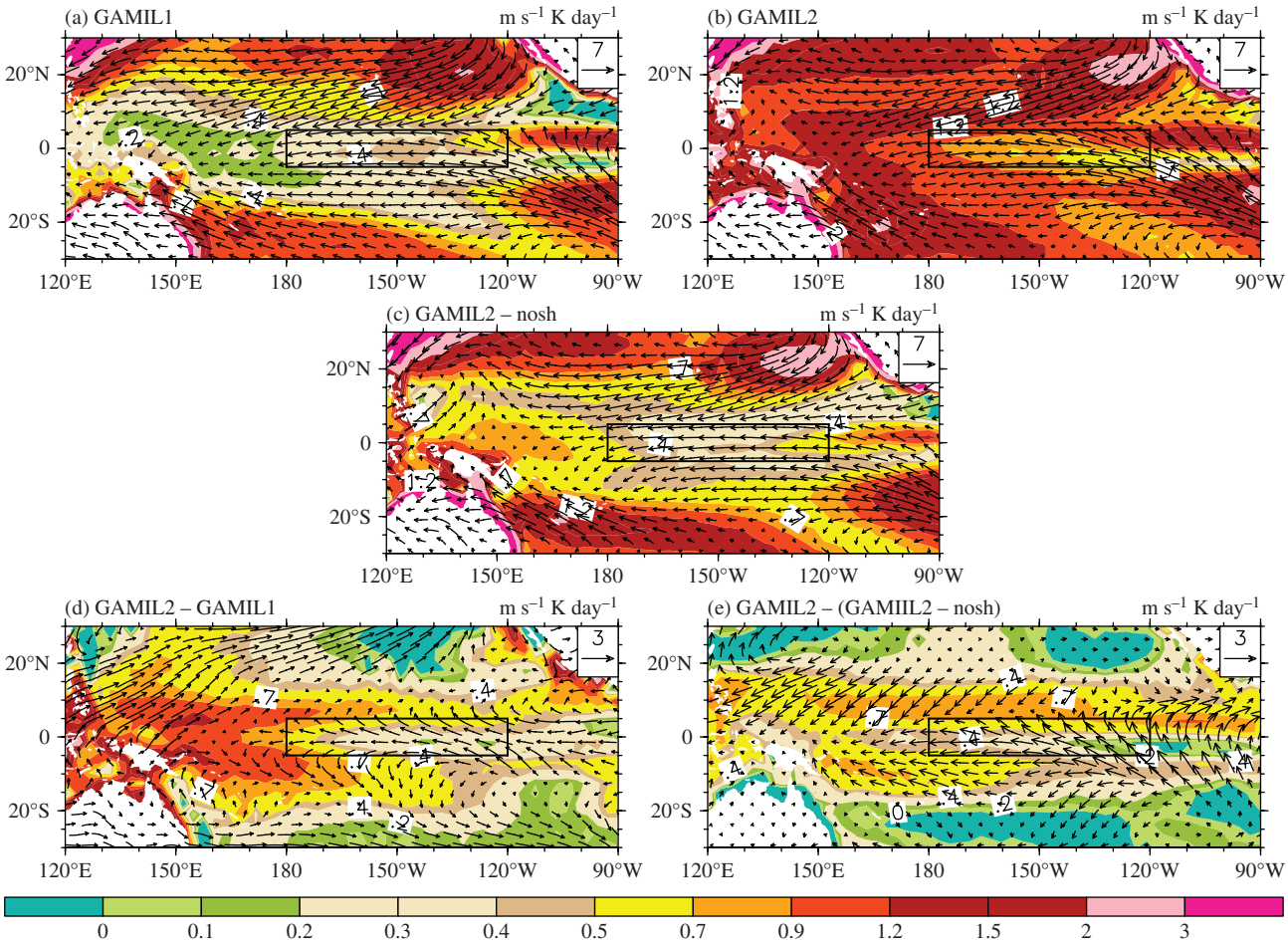


**Figure 3.** Geographic distributions of annual mean wind (vector) and diabatic heating rate (color) at 1000 hPa from (a) GAMIL1, (b) GAMIL2, and (c) GAMIL2-nosh, and the differences between (d) GAMIL2 and GAMIL1, and (e) GAMIL2 and GAMIL2-nosh.

improvement of surface wind, DH, and rainfall simulations needs the improved representation of each physical process and interactions among them.

## 4. Summary and discussion

The direct effect of lower-tropospheric DH on surface circulation over the equatorial Pacific is investigated using the theoretical analysis and three GAMIL simulations. The Matsuno-Gill model shows that the surface winds are directly modulated by the tropical heating gradients. To verify it in models, three simulations are performed only differing in the moist processes, namely, the different deep convective schemes (including the convective cloud) and cloud microphysical processes between GAMIL1 and GAMIL2, and with and without the shallow convection in the tropics in GAMIL2 and GAMIL2-nosh, respectively. Despite the same zonal wind at 850 hPa, GAMIL1 and GAMIL2 display the different surface easterlies, i.e. about 3 m s$^{-1}$ stronger in GAMIL2 than GAMIL1 as well as GAMIL2-nosh and NCEP reanalysis over the central equatorial Pacific and about 3 m s$^{-1}$ weaker in GAMIL1 than GAMIL2 as well as GAMIL2-nosh and ECMWF-interim over the eastern Pacific. Over the eastern Pacific, the westerly biases in GAMIL1 is directly linked to its largest tropical heating increases eastwards at 1000 hPa which reverse the negative SST gradients. Over the central Pacific, the overly strong easterlies in GAMIL2 are from the stronger horizontal tropical heating gradients both in east–west and south–north directions when compared with other two simulations. Furthermore, the similar $u$ at 850 hPa and the different $u$ at 1000 hPa in GAMIL1 and GAMIL2 indicate the surface wind is not sensitive to DH in the middle and high troposphere over the equatorial Pacific; both the same simulations at 850 hPa and diverse simulations at 1000 hPa of zonal wind by GAMIL1 and GAMIL2, and the insensitivity of surface wind to DH above 850 hPa are connected with the vertical disagreement of DH between the layers above and below 925 hPa.

Below the 925-hPa level the cooling from the moist and radiative processes is mostly counterbalanced by the diffusion heating, thus the total heating, as well as surface wind and rainfall, is contributed by each physical process and interactions among them. In addition, given SST, the lower-tropospheric DH gradient is not the only deterministic factor to surface winds, however, the influence of heating distribution on wind perturbation is very important in the lower troposphere. The

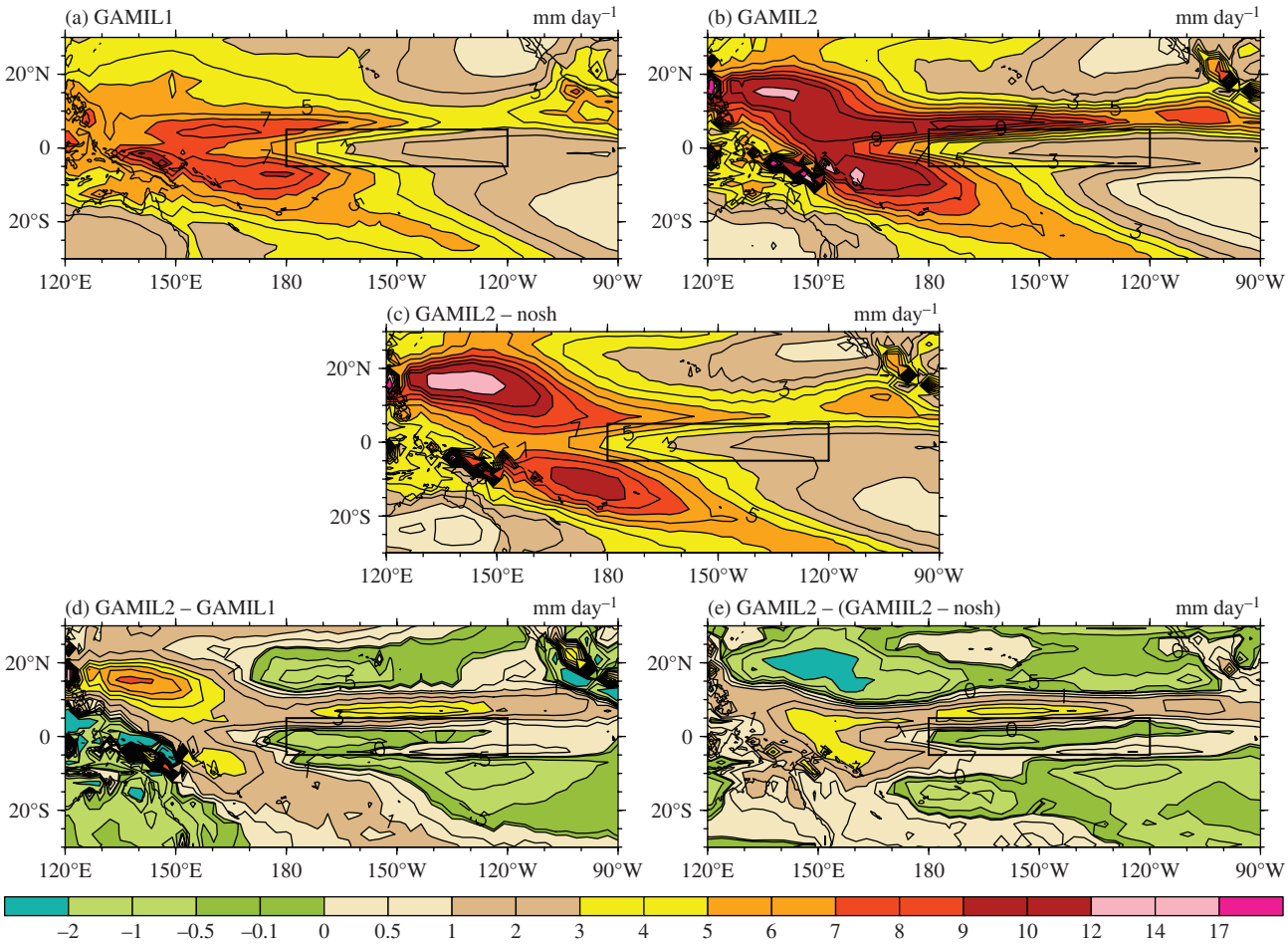


**Figure 4.** Geographic distributions of annual mean rainfall from (a) GAMIL1, (b) GAMIL2, and (c) GAMIL2-nosh, and the differences between (d) GAMIL2 and GAMIL1, and (e) GAMIL2 and GAMIL2-nosh.

influence of the gradients of divergence and convergence on surface wind according to Equation (4) and the agreement between lower-tropospheric DH differences and rainfall differences among three simulations need to be further studied.

## Acknowledgements

This work was supported by the National '973' Project (grant no. 2010CB951904), China Meteorological Administration R & D Special Fund for Public Welfare (meteorology) (grant no. GYHY201006014), and National Natural Science Foundation of China (grant nos. 40923002 and 41005053).

## References

Back LE, Bretherton CS. 2006. Geographic variability in the export of moist static energy and vertical motion profiles in the tropical Pacific. *Geophysical Research Letters* **33**: L17810, doi: 10.1029/2006GL026672.

Cai Q, Zhang GJ, Zhou T. 2013. Impacts of shallow convection on MJO simulation: a moist static energy and moisture budget analysis. *Journal of Climate* **26**: 2417–2431, doi: 10.1175/JCLI-D-12-00127.1.

Chan SC, Nigam S. 2009. Residual diagnosis of diabatic heating from ERA-40 and NCEP reanalyses: intercomparisons with TRMM. *Journal of Climate* **22**: 414–428.

Chang CY, James AC, Grodsky SA, Nigam S. 2007. Seasonal climate of the tropical Atlantic sector in the NCAR Community Climate System Model 3: error structure and probable causes of errors. *Journal of Climate* **20**: 1053–1070.

Chang CY, Nigam S, James AC. 2008. Origin of the springtime westerly bias in equatorial atlantic surface winds in the community atmosphere model version 3 (CAM3) simulation. *Journal of Climate* **21**: 4766–4778, doi: 10.1175/2008JCLI2138.1.

Chiang JCH, Zebiak SZ, Cane MA. 2001. Relative roles of elevated heating and surface temperature gradients in driving anomalous surface winds over the tropical oceans. *Journal of the Atmospheric Sciences* **58**: 1371–1394.

DeWitt D. 2005. Diagnosis of the tropical Atlantic near-equatorial SST bias in a directly coupled atmosphere–ocean general circulation model. *Geophysical Research Letters* **32**: L01703, doi: 10.1029/2004GL021707.

Gill AE. 1980. Some simple solutions for heat-induced tropical motion. *Quarterly Journal of the Royal Meteorological Society* **449**: 447–462.

Guilyardi E, Wittenberg A, Fedorov A, Collins M, Wang CZ, Capotondi A, Oldeborgh GJ, Stockdale T. 2009. Understanding El Niño in ocean-atmosphere general circulation models: progress and challenges. *Bulletin of the American Meteorological Society* **90**: 325–340.

Hagos S, Zhang CD, Tao WK, Lang S, Takayabu YN, Shige SC, Katsumata M, Olson B, L'Ecuyer T. 2010. Estimates of tropical diabatic heating profiles: commonalities and uncertainties. *Journal of Climate* **23**: 542–558.

Kanamitsu M, Ebisuzaki W, Woolen J, Yang SK, Hnilo JJ, Fioriono M, Potter GL. 2002. NCEP-DOE AMIP-II Reanalysis (R-2). *Bulletin of the American Meteorological Society* **83**: 1631–1643.

Kumar BP, Vialard J, Lengaigne M, Murty VSN, McPhaden MJ, Cronin MF, Pinsard F, Reddy KG. 2013. TropFlux wind stresses over the tropical oceans: evaluation and comparison with other products. *Climate Dynamics* **40**: 2049–2071.

Li LJ, Wang B. 2010. Influences of two convective schemes on the radiative energy budget in GAMIL1.0. *Acta Meteorologica Sinica* **24**(3): 318–327.

Li LJ, Xie X, Wang B, Dong L. 2012. Evaluating the performances of GAMIL1.0 and GAMIL2.0 during TWP-ICE with CAPT. *Atmospheric and Oceanic Science Letters* **5**: 38–42.

Li LJ, Lin PF, Yu YQ, Wang B, Zhou TJ, Liu L, Liu J, Bao Q, Xu SM, Huang WY, Xia K, Pu Y, Dong L, Shen S, Liu YM, Hu N, Liu MM, Sun WQ, Shi XJ, Zheng WP, Wu B, Song MR, Liu HL, Zhang XH, Wu GX, Xue W, Huang XM, Yang GW, Song ZY, Qiao FL. 2013a. The flexible global ocean-atmosphere-land system model version g2. *Advances in Atmospheric Sciences* **30**(3): 543–560, doi: 10.1007/s00376-012-2140-6.

Li LJ, Wang B, Dong L, Liu L, Shen S, Hu N, Sun WQ, Wang Y, Huang WY, Shi XJ, Pu Y, Yang GW. 2013b. Evaluation of Grid-point Atmospheric Model of IAP LASG, Version 2.0 (GAMIL 2.0). *Advances in Atmospheric Sciences* **30**(3): 855–867, doi: 10.1007/s00376-013-2157-5.

Li LJ, Wang B, Zhang GJ. 2014. The role of non-convective condensation processes in response of surface shortwave cloud radiative forcing to El Niño warming. *Journal of Climate*, doi: 10.1175/JCLI-D-13-00632.1.

Ling J, Zhang C. 2011. Structural evolution in heating profiles of the MJO in global reanalyses and TRMM retrievals. *Journal of Climate* **24**: 825–842.

Ling J, Zhang C. 2013. Diabatic heating profiles in recent global reanalyses. *Journal of Climate* **26**: 3307–3325, doi: 10.1175/JCLI-D-12-00384.1.

Matsuno T. 1966. Quasi-geostrophic motion in the equatorial area. *Journal of the Meteorological Society of Japan* **44**(1): 25–43.

Morrison H, Gettelman A. 2008. A new two-moment bulk stratiform cloud microphysics scheme in the Community Atmosphere Model, version 3 (CAM3). Part I: description and numerical tests. *Journal of Climate* **21**(15): 3642–3659.

Nigam S, Chung C. 2000. ENSO surface winds in CCM3 simulation: diagnosis of errors. *Journal of Climate* **13**: 3172–3186.

Rasch PJ, Kristjánsson JE. 1998. A comparison of the CCM3 model climate using diagnosed and predicted condensate parameterizations. *Journal of Climate* **11**(7): 1587–1614.

Schumacher C, Houze JRA, Kraucunas I. 2004. The tropical dynamical response to latent heating estimates derived from TRMM precipitation radar. *Journal of the Atmospheric Sciences* **61**: 1341–1358.

Simmons A, Uppala S, Dee D, Kobayashi S. 2006. ERA-Interim: new ECMWF reanalysis products from 1989 onwards. *ECMWF Newsletter* **110**: 26–35.

Wang B, Wang H, Ji ZZ, Zhang X, Yu RC, Yu YQ, Liu HT. 2004. Design of a new dynamical core for global atmospheric models based on some efficient numerical methods. *Science in China Series A: Mathematics* **47**: 4–21.

Wright JS, Fueglistaler S. 2013. Large differences in reanalyses of diabatic heating in the tropical upper troposphere and lower stratosphere. *Atmospheric Chemistry and Physics* **13**: 9565–9576.

Wu ZH. 2003. A shallow CISK, deep equilibrium mechanism for the interaction between large-scale convection and large-scale circulations in the tropics. *Journal of the Atmospheric Sciences* **60**: 377–392.

Xu KM, Krueger SK. 1991. Evaluation of cloudiness parameterizations using a cumulus ensemble model. *Monthly Weather Review* **119**: 342–367.

Yu RC. 1994. A two-step shape-preserving advection scheme. *Advances in Atmospheric Sciences* **11**: 479–490.

Zermeño-Diaz DM, Zhang CD. 2013. Possible root causes of surface westerly biases over the equatorial Atlantic in global climate models. *Journal of Climate* **26**: 8154–8168, doi: 10.1175/JCLI-D-12-00226.1.

Zhang CD, Hagos SM. 2009. Bi-modal structure and variability of large-scale diabatic heating in the tropics. *Journal of the Atmospheric Sciences* **66**: 3621–3640.

Zhang GJ, McFarlane NA. 1995. Sensitivity of climate simulations to the parameterization of cumulus convection in the Canadian Climate Centre general circulation model. *Atmosphere-Ocean* **33**: 407–446.

Zhang GJ, Mu M. 2005. Effects of modifications to the Zhang-McFarlane convection parameterization on the simulation of the tropical precipitation in the National Center for Atmospheric Research Community Climate Model, version 3. *Journal of Geophysical Research* **110**: D09109.

Zhang GJ, Song X. 2009. Interaction of deep and shallow convection is key to Madden-Julian Oscillation simulation. *Geophysical Research Letters* **36**: L09708, doi: 10.1029/2009GL037340.

 